Water Research 248 (2024) 120856

Contents lists available at ScienceDirect

Water Research

journal homepage: www.elsevier.com/locate/watres

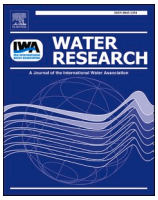

Transitioning through the vapour-liquid equilibrium for low energy thermal stripping of ammonia from wastewater: Enabling transformation of NH_3 into a zero-carbon fuel

B. Luqmani [a], A. Brookes [b], A. Moore [c], P. Vale [d], M. Pidou [a], E.J. McAdam [a,*]

[a] Cranfield Water Science Institute, Vincent Building, Cranfield University, Bedfordshire MK43 0AL, UK
[b] Anglian Water, Block C-Western House, Peterborough Business Park, Peterborough PE2 6FZ, UK
[c] Northumbrian Water, Boldon House, Wheatlands Way, Durham DH1 5FA, UK
[d] Severn Trent Water, 2 St. Johns Street, Coventry CV1 2LZ, UK

ARTICLE INFO

Keywords:
Ammonia to energy
Vacuum stripping
Net zero
Resource recovery
Wastewater

ABSTRACT

Vacuum thermal stripping permits the recovery of ammonia from wastewater in a concentrated form, which is key to its exploitation in the circular economy, but the latent heat demand for thermal separation remains a critical barrier to exploitation. In this study, we investigate the vapor-liquid equilibrium (VLE) for ammonia-water as a mechanism to enhance recovered ammonia quality and minimise the thermal energy required for ammonia separation. Below the dew point (65 °C at 0.25 bar) a two-phase region of the VLE exists where 48 %wt gas-phase ammonia could be produced (61 °C) compared to only 2 %wt within the stripping region adopted widely in the literature. This was complemented by a 98 % reduction in thermal separation energy, since limited water vaporization can occur when the feed is maintained below the activation energy threshold for bulk evaporation. Operation within this practically unexplored region of the ammonia-water VLE fosters a gas-phase product suitable for energy generation in gas turbines or solid oxide fuel cells. Comparable product quality was achieved using concentrated wastewater, which validated the VLE for design in the presence of a broad range of dissolved gases and volatile inorganic compounds. Rapid desorption of CO_2 occurred during vacuum stripping, subsequently increasing pH >9 without the requirement for alkali addition to shift the ammonia-ammonium equilibrium in favor of gaseous ammonia. Consequently, the two-phase region of the VLE defined for vacuum thermal stripping provides a synergistic strategy to mitigate chemical demand, minimise separation energy and recover gas-phase ammonia for zero carbon energy generation, constituting a significant advancement toward the net zero ambitions of the water sector.

1. Introduction

Ammonia in municipal wastewater is removed by biological oxidation in the activated sludge process. Ammonia oxidation consumes 3-5 $kWh_e\ kg_N^{-1}$ for forced aeration and can represent 20 % of the total energy demand for wastewater treatment (Garrido et al., 2013; Wett, 2006). During ammonia oxidation, 0.3 % of the nitrogen is transformed into nitrous oxide (N_2O) which has a global warming potential 310-times greater than CO_2 (Campos et al., 2016; Winter et al., 2012). Consequently, ammonia removal is associated with almost half of greenhouse gas (GHG) emissions in wastewater treatment (Campos et al., 2016). To improve environmental standards and public health, nitrogen limits for treated wastewater in Europe are reducing to 10 mg L^{-1} (for works serving >0.1 million P.E.) within the Urban Wastewater Treatment Directive 91/271/EEC (EEC Council, 1991). The new discharge standards will require higher nitrogen removal from existing wastewater treatment processes, or prompt investment to expand treatment capacity, which will increase energy demand and GHG emissions associated with ammonia removal.

Ammonia recovery from wastewater is an opportunity to advance sustainability within the water sector. Currently, approximately 185 Mtonnes y^{-1} of ammonia is synthesised in the energy intensive Haber-Bosch process (19 $kWh_{th}\ kg_N^{-1}$) to meet agricultural and industrial demands (Mission Possible Partnership, 2022; Morgan, 2013). Ammonia synthesis is presently 95 % reliant on fossil-fuel derived hydrogen feedstocks and is consequently associated with 1.3 % of global CO_2

* Corresponding author.
E-mail address: e.mcadam@cranfield.ac.uk (E.J. McAdam).

https://doi.org/10.1016/j.watres.2023.120856
Received 18 August 2023; Received in revised form 7 November 2023; Accepted 9 November 2023
Available online 10 November 2023

emissions (International Energy Agency, 2021; Nayak-Luke et al., 2018). The demand for ammonia is projected to expand to at least 255 Mtonnes y^{-1} by 2050 due to the rising global population and this has stimulated interest in decarbonising its production (International Energy Agency, 2021; Mission Possible Partnership, 2022). This could be achieved by incorporating carbon capture and storage for 'blue' ammonia production, or a transition to electrified plants powered by renewable energy sources for 'green' ammonia production (Cesaro et al., 2021; Morgan, 2013). Across the UK water sector alone, there is an opportunity to recover up to 400 tonnes of sustainable ammonia per day which could offset commercial ammonia production and therefore align directly with existing objectives for industrial decarbonisation (Henze and Comeua, 2008; Parliamentary Office of Science and Technology, 2007).

Many researchers have focussed on ammonia recovery from wastewater to produce agricultural fertilisers (i.e., ammonium sulphate, struvite) (Vaneeckhaute et al., 2017). There are complex barriers to the sale of fertiliser produced from wastewater since it is classified as waste under the European Waste Framework Directive 2008/98/EC (EC, 2008). With a lower heating value of 5.3 kWh kg^{-1} (comparable to biogas, 6.1 kWh kg^{-1}), ammonia is also emerging as a next generation zero carbon fuel (Table 1) (Moore and Auty, 2013; The Royal Society, 2020). As the water sector is already strongly focused on renewable energy production, ammonia can therefore provide significant value. For example, biogas turbines used for combined heat and power (CHP) generation are often co-located with ammonia-rich digested sludge liquors. Gas-phase ammonia recovery could support the co-combustion of an ammonia/biogas mixture to increase energy production (Kurata et al., 2017; Okafor et al., 2021). Gaseous, aqueous or anhydrous liquified ammonia can also be consumed in fuel cells that are not limited to classical Carnot inefficiencies and thus achieve electrical efficiencies greater than those of existing CHP engines (>50 %) (Lan and Tao, 2014; The Royal Society, 2020). Ammonia can also be 'cracked' electrolytically or catalytically to produce hydrogen (Jackson et al., 2015; Vitse et al., 2005), directly in line with ongoing investment into hydro-powered hydrogen production within the water sector to access an expanding hydrogen economy (Anglian Water, 2021; Department for Business, Energy and Industrial Strategy, 2021). Ammonia to energy could therefore reduce energy importation for water utilities and limit exposure to volatile energy prices or create new revenue streams through the exportation of hydrogen-based zero carbon fuels. The capability to meet stringent nitrogen discharge limits, reductions in GHG emissions and grid based power, while producing a zero carbon fuel creates a holistic strategy for the water sector that resonates with its broader net zero ambitions (Water Europe, 2021; Water UK, 2020). However, the concentration, purity and form (i.e., aqueous or gas) that the ammonia is recovered in will determine the available routes for its exploitation as a zero carbon fuel (Table 1).

Since ammonia is relatively dilute and contained within the complex wastewater matrix, its separation and purification from wastewater is required to capitalise on ammonia to energy opportunities. In a centralised wastewater treatment works, 20-40 %wt of the ammonia load is concentrated within centrifuged liquors originating from anaerobic digestion (centrate) which represent less than 1 % of the treatment flow (Ndam, 2017). This low-volume sidestream presents an ideal target for economic ammonia recovery, since the raised concentration will enhance the driving force for ammonia mass transfer during stripping (Bavarella et al., 2020; Ukwuani and Tao, 2016). Air and steam stripping are already commercially established (Organics Group, 2020; RVT, 2015). High gas-liquid ratios (>2500 m^3_{gas} m^{-3}_{liquid}) are necessary during air stripping which generates dilute gas-phase ammonia (<0.05 %wt NH_3) (Huang and Shang, 2006; Jiang, 2009). Operating at high temperatures will reduce ammonia solubility, and so steam stripping requires lower gas-liquid ratios (<300 m^3_{gas} m^{-3}_{liquid}) and generates an ammonia vapor at higher purity (0.5-2.0 %wt) but the thermal demand increases to ~150 kWh_{th} kg_N^{-1} primarily due to the latent heat demand for raising steam (Teichgraber and Stein, 1994; Zeng et al., 2006). As existing stripping solutions are primarily used for abatement, gas-phase ammonia is generally oxidised at high temperatures over a catalyst (250-450 °C), or captured in sulphuric acid to produce a relatively dilute ammonium sulphate solution that requires disposal (Huang and Shang, 2006; Jamaludin et al., 2018; Wang et al., 2021). To improve the viability of zero carbon energy production from wastewater ammonia, stripping technologies must be able to produce aqueous ammonia or anhydrous liquified ammonia products in sufficient concentration to meet the needs of emergent energy applications. The separation and purification of ammonia must also be achieved with minimal energy input to maximise the potential for this new resource.

Vacuum thermal stripping is an emerging alternative, demonstrated at laboratory scale, in which wastewater is heated to saturation in a partial vacuum (Bavarella et al., 2020; Han et al., 2022). The absolute temperature for boiling reduces with the vacuum pressure applied. Consequently, the thermal energy demand can be reduced, enabling the integration of low-grade waste heat sources (Anwar and Tao, 2016). In a centralised wastewater treatment works, 47 kWh_{th} of low-grade waste heat at modest quality (85 °C in water) could be recovered from biogas turbines per m^3 of centrate (Moore and Auty, 2013; Ndam, 2017). Ammonia has a higher volatility than water and so the vapors produced during boiling will be relatively rich in ammonia compared to the

Table 1
Technologies for energy and hydrogen generation using ammonia.

Application	Ammonia state	Ammonia purity %wt	Electrical efficiency %LHV	Heat generation %LHV	Heat quality -
Gas turbine[a]	Gaseous[b]	>20%[b,d]	30-40%[c,d]	60-70%	>400 °C [d,l]; <100 °C [d,l]
SOFC	Gas[d,e]	>5%[e,f]	50-70%[c,f]	30-50%	>700 °C[g]
Low temperature AFC	Aqueous / Gas[h,i]	<0.01% [h,i]	50-60%[c,i]	-	-
Cracking to H_2	Gas[j]	>5%[e,f,j]	-	-	-
Electrolysis to H_2	Aqueous[k]	<0.01%[k]	-	-	-

LHV – Lower heating value for ammonia (5.3 kWh kg^{-1}); AFC – alkaline fuel cell; SOFC – solid oxide fuel cell.
[a] Ammonia-fed or co-fueled with methane.
[b] (Kurata et al., 2017; Okafor et al., 2021a).
[c] (The Royal Society, 2020).
[d] (Hewlett et al., 2020, 2019).
[e] (van Linden et al., 2022).
[f] (Dekker and Rietveld, 2006).
[g] (Patel et al., 2012).
[h] (Zhang et al., 2020).
[i] (Siddiqui and Dincer, 2019a).
[j] (Jackson et al., 2015).
[k] (Cooper and Botte, 2006; Vitse et al., 2005).
[l] ~50% high-grade and ~50% low grade heat.

liquid-phase (Pátek and Klomfar, 1995; Ukwuani and Tao, 2016). These vapors are continously extracted by the vacuum pump, which enhances the volumetric mass transfer coefficient and maintains the driving force for ammonia mass transfer across the gas-liquid interface (Han et al., 2022). While several studies on vacuum stripping are reported, there is limited data on the composition of the vapor product. Bavarella et al. (2020) applied vacuum thermal stripping to a 7.5 kg m^{-3} aqueous ammonia feed and condensed the vapors to produce a 101 kg m^{-3} aqueous ammonia product. While the concentration factor compares favorably to air and steam stripping, the product is below the specification generally required for energy production, implying that further purification stages are required (e.g., distillation). The product quality also indicates substantial evaporation of water from the feed during stripping. This will incur a high latent heat penalty which can represent over 90 % of the total energy consumption for ammonia removal (Davey et al., 2022). Consequently, further selectivity toward ammonia must be fostered during the separation to improve the economic and environmental viability for vacuum thermal stripping in wastewater treatment.

Fundamentally, vacuum thermal stripping is a distillation process since it exploits the difference in volatility between ammonia and water (Ukwuani and Tao, 2016; van Linden et al., 2022). In a binary ammonia-water mixture, the fraction of ammonia in the liquid and vapor phase at a specific temperature are related by the vapor-liquid equilibrium (VLE). A model has been developed for estimation of the ammonia-water VLE based on regression analysis of meta-data for absorption refrigeration from 0.5-20 bar (Fig. 1) (Pátek and Klomfar, 1995). Separation of ammonia and water will occur in the two-phase region bounded by the bubble and dew point curves. When the liquid-phase (x_f) is heated close to the upper boundary of the two-phase region (T_1), a substantial fraction of ammonia will be released into the gas-phase at equilibrium to leave a dilute final solution (x_1). This will produce a vapor phase which has a greater ammonia concentration than the initial liquid phase (y_1). Alternatively, when the liquid-phase is heated close to the lower boundary of the two-phase region (T_2), a smaller fraction of ammonia is released from the feed (x_2). However, there will be an enhancement in selectivity for ammonia transport (the more volatile component) relative to water. Consequently, the vapor phase will exhibit a greater ammonia concentration than can be achieved at T_1. Based on the existing boundaries which have been theoretically derived for the VLE, we can postulate that the extraction of the vapor phase during vacuum thermal stripping will continuously reset this equilibrium and cause the liquid-phase ammonia concentration to decline over time. Hence, a stripping process at T_1 will achieve rapid ammonia mass transfer, whilst operating at T_2 will produce high purity vapor but at a limited mass transfer rate. A purer vapor phase could be directly applied for energy generation, obviating the capital cost and energy requirements related to the downstream purification of ammonia. Further, it would be associated with a lower fraction of water vaporization from the feed, thereby minimising latent heat demand for the process and increasing the energy efficiency for ammonia recovery. Controlling temperature and pressure to achieve a setpoint within the two-phase region may therefore introduce a disruptive breakthrough for thermal stripping, by delivering an ammonia product at maximum concentration and with minimum separation energy.

However, in the majority of research published on vacuum thermal stripping of wastewater, a vacuum pressure of 0.25-0.27 bar and a uniform temperature of 65 °C has been applied independently of the feed concentration. The experimental conditions were selected to achieve vigorous boiling in the feed, and when overlaid onto the VLE, evidence that the system was operated close to its dew point (65.1-65.3 °C) (Fig. 2). Consequently, despite the prospective benefits to separation energy and product purity, the two-phase region has not been explored to date. Crucially, concentrated wastewater (x_{NH3}<0.002) at 0.25 bar exists at the lower limit of the VLE, which has not been well characterized historically within the literature, since the focus has been on ammonia-water refrigeration mixtures (typically x_{NH3}>0.5) (Ganesh and Srinivas, 2017; Raghuvanshi and Maheshwari, 2011). Prediction of the two-phase region using extrapolated data may be particularly challenging due to solvent-solute interactions between ammonia and water which can influence the VLE (Tan et al., 2004). The precise width of the two-phase region relevant for ammonia stripping from wastewater is therefore uncertain, and experimental characterization is necessary to establish the extent to which ammonia-water selectivity can be controlled during ammonia stripping. The aim of this study was to characterize the ammonia-water separation mechanism during vacuum thermal stripping and investigate the potential to exploit the two-phase region to increase ammonia selectivity and facilitate low-energy, high purity ammonia recovery from wastewater. Specific objectives were to:

I benchmark ammonia separation in vacuum thermal stripping through initially characterizing selectivity at the dew point to compare against existing literature;
II transition from the dew point through the two-phase region to determine the extent to which ammonia-water selectivity can be manipulated;

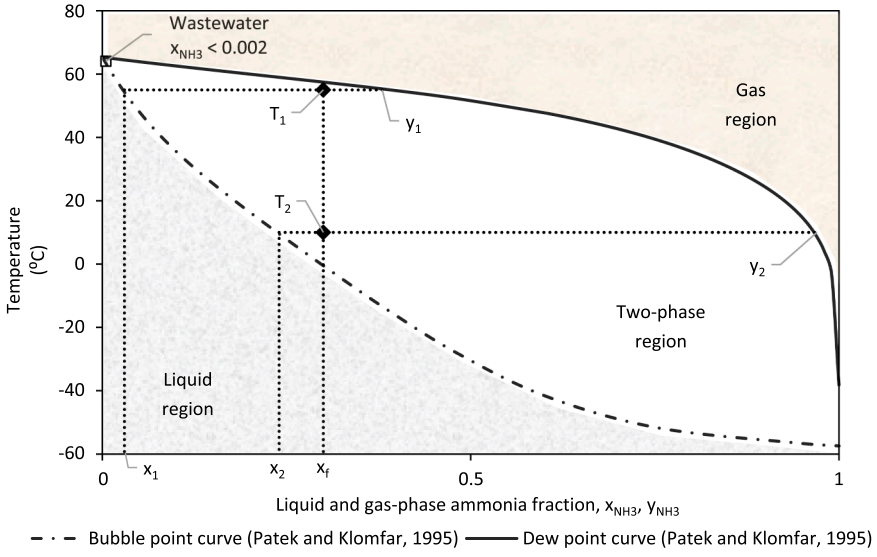

Fig. 1. VLE for NH_3-H_2O at 0.25 bar defined using empirical method Eqs. (12) and ((13))

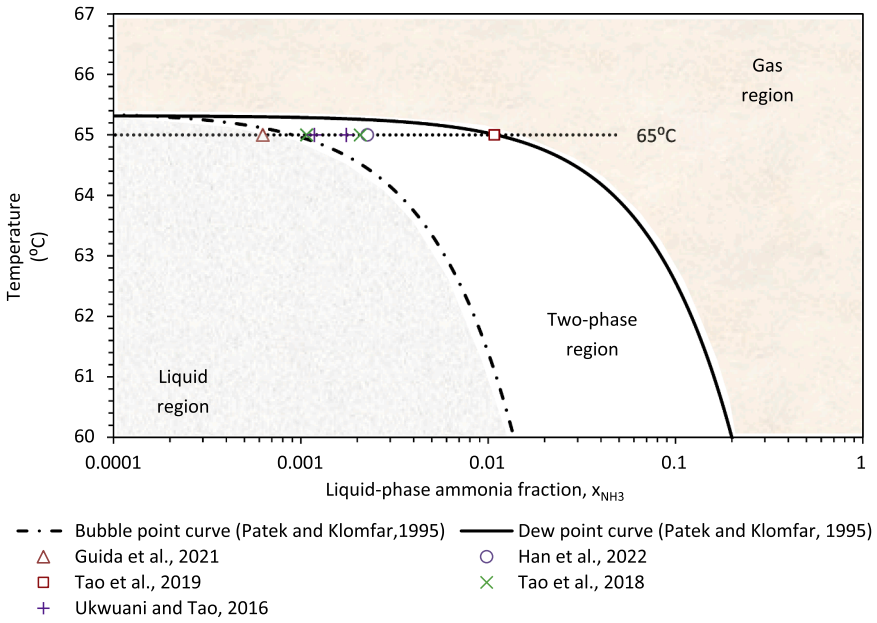

Fig. 2. Operating points for vacuum thermal stripping of real and synthetic wastewater at 0.25-0.27 bar in previous work, placed within the context of the NH_3-H_2O VLE Eqs. (12) and ((13)).

III consider the potential for enhanced ammonia selectivity during stripping as an enabler for ammonia to energy strategies in wastewater treatment;
IV characterize stripping performance using concentrated wastewater to investigate the impact of dissolved volatile compounds and gases on the ammonia-water separation;
V explore the potential for chemical-free vacuum thermal stripping to complement and enhance the prospective energy and cost benefits when operating within the two-phase region.

2. Materials and methods

2.1. Experimental set-up

Vacuum thermal stripping experiments were conducted in a batch system developed at laboratory scale (Fig. 3). In each experiment, 0.5 kg of feed was placed in a 1 L jacketed vessel and agitated using a magnetic stirrer at approximately 450 rpm (SB151, Stuart Ltd., Stone, UK). The feed was heated to 61, 63 or 65 ±0.5 °C at atmospheric pressure (MPC-K6, Huber, Offenburg, Germany). When the target temperature was achieved, system pressure was reduced to 0.25 bar using a vacuum pump in combination with a vacuum control valve (ME-1C, Vacuubrand, Wertheim, Germany; SS-4MA-MH, Swagelok, Kings Langley, UK). Stripping temperature and pressure were monitored continuously (Type K, RS Components, Corby, UK; PXM319-010GI, Omega Engineering Ltd, Manchester, UK). Ammonia-rich vapor stripped from the feed was drawn through a condenser operated at 3-5 °C with 250 cm^2 surface area (Quickfit C6/12/SC, Fisher Scientific, Loughborough, UK; LT Ecocool 150, Grant Instruments, Cambridge, UK). Condensate was stored in a chilled, jacketed vessel at 3-5 °C to prevent further ammonia

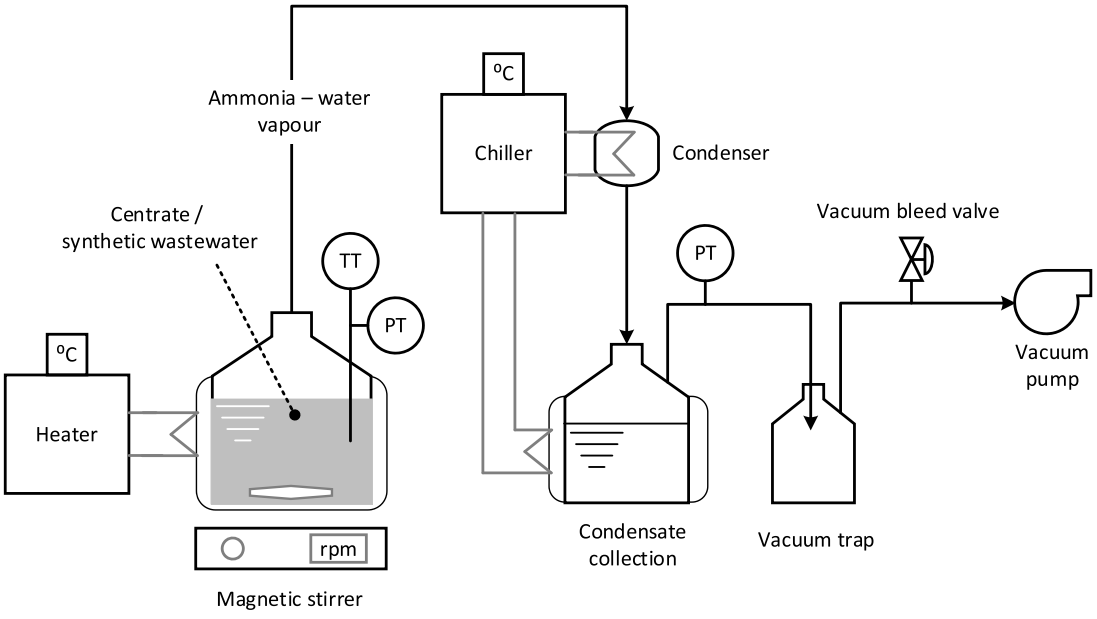

Fig. 3. Schematic of the vacuum thermal stripping experiment. TT and PT represent temperature and pressure transmitters, respectively.

stripping. Each primary data point was collected in duplicate or triplicate. Standard deviation is represented by error bars.

2.2. Wastewater preparation and analysis

Synthetic wastewater containing 1.5 g L^{-1} ammonia was produced using deionised water (15 MΩ cm) and ammonium hydroxide (35 %wt, Fisher Scientific, Loughborough, UK). Centrifuged sludge liquors originating from conventional anaerobic digestion (Centrate A) and advanced anaerobic digestion (Centrate B) were sampled from separately located wastewater treatment works in England (Table 2). Sodium hydroxide was added to amend pH as required (97 %wt pearl, Fisher Scientific, Loughborough, UK). Ammoniacal nitrogen and chemical oxygen demand (COD) was determined using spectrophotometry with proprietary cell tests (114558 & 114559 NH_4-N, 11451 COD, Spectroquant cell tests, Merck-Millipore, Darmstadt, Germany). For the centrate and distillate, soluble COD was determined following 0.45 μm syringe filtration (Whatman, Maidstone, UK), whilst pH measurement was conducted in a temperature-controlled environment at 21 °C (InPro 3250i/SG/120, Mettler-Toledo Ltd, Leicester, UK). Standard methods 2540B and 2540D were applied to determine total solids, suspended solids and dissolved solids (APHA/AWWA/WEF, 2012). Centrate alkalinity was determined by titration with hydrochloric acid (37 %, Fisher Scientific, Loughborough, UK). Total inorganic carbon content (TIC) was analysed using a TOC analyser (Shimadzu, Milton Keynes, UK).

2.3. Experimental analysis

Ammonia will partially dissociate in wastewater to form non-volatile ammonium:

$$NH_{3(aq)} + H^{+}_{(aq)} \leftrightarrow NH^{+}_{4(aq)} \quad (1)$$

The fraction of free ammonia in the feed can be estimated from the pH and temperature (Eqs. (2) and (3); Fig. A1):

$$\Phi = \frac{1}{1 + 10^{(pK^{s}_{a,T} - pH)}} \quad (2)$$

$$pK^{s}_{a,\,T} = pK^{s}_{a,298} + 0.0324\ [298.15 - T)] \quad (3)$$

where Φ is the fraction of free ammonia (-); $pK^{s}_{a,298}$ and $pK^{s}_{a,T}$ are the negative logarithm of the acid dissociation constant at 298 K and T (K), respectively [-]. The estimation of free ammonia Eqs. (2) and ((3)) is based on aqueous ammonia dissociation constants that were derived experimentally (Bates and Pinching, 1949,1950). The validity of these dissociation constants was confirmed through comparison with the fundamental approach of van't Hoff:

$$ln\frac{K_1}{K_2} = \frac{\Delta H^{0}_{rxn}}{R}\left(\frac{1}{T_1} - \frac{1}{T_2}\right) \quad (4)$$

Table 2
Characterization of centrate used in this work, produced from full-scale AD facilities treating municipal wastewater sludge.

Parameter	Centrate A	Centrate B[a]
Origin	Conventional AD	Advanced AD[b]
Ammonia concentration, C_{NH3} (g L^{-1})	1.0	2.0
pH (-)	7.8	8.0
Total COD (g L^{-1})	1.2	5.8
Soluble COD (g L^{-1})	0.4	0.3
Total suspended solids (g L^{-1})	0.2	0.3
Total dissolved solids (g L^{-1})	1.6	4.6
Total inorganic carbon (as C) (g L^{-1})	1.0	1.7
Alkalinity (as $CaCO_3$) (g L^{-1})	3.7	6.9

AD – anaerobic digestion; COD – chemical oxygen demand.
[a] Characterization originally published by Davey et al. (2022)
[b] Raw sludge pre-treated by thermal hydrolysis prior to anaerobic digestion.

where ΔH^{0}_{rxn} is the enthalpy of reaction (-51965 J $mole^{-1}$) and R is the universal gas constant (8.314 J K^{-1} $mole^{-1}$) (Puigdomenech et al., 1997). The free ammonia fractions determined by direct measurement (Bates and Pinching, 1949,1950) and those of the fundamental approach (van't Hoff) were within 2 % across the temperature range studied (Appendix A2, Fig. A6). Eq. (2) therefore provides an empirical representation of the fundamental equation in log10 space.

Ammonia mass transfer across the gas-liquid interface can be described by the Lewis-Whitman model (Eq. 5) (Heile et al., 2017; Tao and Ukwuani, 2015). The equilibrium concentration for dissolved ammonia (C_{NH3}*) approaches zero under vacuum conditions across all temperatures applied in this work (Salavera et al., 2005; Ukwuani and Tao, 2016). Integration of Eq. (5) from time = 0 to time = t provides a straight-line function in which the gradient represents the volumetric mass transfer coefficient (k_La) (Eq. (6)).

$$\frac{dC_{NH3}}{dt} = k_L\, a\, \left(\Phi C_{NH3} - C^{*}_{NH3}\right) \quad (5)$$

$$-\ln\left(\frac{C_{NH3,t}}{C_{NH3,0}}\right) = k_L\, a\, t \quad (6)$$

where dC_{NH3}/dt is the rate of ammonia transfer across the gas-liquid interface (g L^{-1} h^{-1}); k_L is the mass transfer coefficient for ammonia (m h^{-1}); a is the specific interfacial area (m^2 m^{-3}); C_{NH3} is the dissolved ammonia concentration (g L^{-1}); Φ is the fraction of free ammonia (-); t is stripping time (h); and subscripts *0* and *t* represent time = 0 and time = t.

During vacuum thermal stripping, the concentration of ammonia in the feed and the total condensate mass were recorded over time. This enabled a mass balance to determine ammonia removal from the feed Eqs. (7)-((9)) and the ammonia mass fraction within the stripped vapor at any time (Eq. (10)). It was assumed that all stripped water was captured by condensation at 3-5 °C and the feed density was equal to that of pure water at the operating temperature due to its dilute nature ($x_{NH3} < 0.002$).

$$V_0 = \frac{m_0}{\rho} \quad (7)$$

$$V_t = \frac{(m_0 - m_{c,t})}{\rho} \quad (8)$$

$$\eta_{NH3} = \frac{C_{NH3,0}V_0 - C_{NH3,t}V_t}{C_{NH3,t}V_t} \quad (9)$$

$$y_{NH3,wt} = \frac{C_{NH3,0}\ V_0 - C_{NH3,t}\ V_t}{m_{c,t}} \quad (10)$$

where V is the feed volume (L); m is the feed mass (g); m_c is the condensate mass (g); and ρ is the feed density (g L^{-1}); η_{NH3} is ammonia removal from the feed (%wt); $y_{NH3,wt}$ is the mass fraction of ammonia in the stripped vapor (%wt).

Ammonia selectivity during stripping could be estimated using the equilibrium pressures of ammonia and water in the feed at the stripping condition and could be experimentally measured based on the relative amounts of ammonia and water removed from the feed over time:

$$\alpha_{NH3} = \frac{p_{NH3}}{p_{H2O}} = \frac{mol_{NH3}}{mol_{H2O}} \quad (11)$$

where α_{NH3} is the selectivity for ammonia during stripping (bar_{NH3} bar^{-1}_{H2O}or mol_{NH3} mol^{-1}_{H2O}); p_{NH3} and p_{H2O} represent the equilibrium vapor pressures of ammonia and water, respectively (bar); and mol_{NH3} and mol_{H2O} represent the amount of ammonia and water removed from the feed, respectively (moles).

The empirical dew and bubble point curves for the ammonia-water system were computed at 0.25 bar Eqs. (12)-((13)) (Pátek and Klomfar, 1995):

$$T_b(P,\ x_{NH3}) = T_0 \sum_i a_i (1 - x_{NH3})^{m_i} \left[ln\left(\frac{P_0}{P}\right) \right]^{n_i} \quad (12)$$

$$T_d(P,\ y_{NH3}) = T_0 \sum_i a_i (1 - y_{NH3})^{\frac{m_i}{4}} \left[ln\left(\frac{P_0}{P}\right) \right]^{n_i} \quad (13)$$

where T_b is the bubble temperature (K) of the ammonia-water mixture at the applied pressure P (0.25 bar) for a liquid-phase containing an ammonia mole fraction of x_{NH3} (-); T_d is the dew temperature (K) of the ammonia-water mixture at P for a vapor phase containing an ammonia mole fraction of y_{NH3} (-); T_0 is the reference temperature (100 K); P_0 is the reference pressure (20 bar); a_i, m_i and n_i are empirical coefficients (Pátek and Klomfar, 1995).

3. Results and discussion

3.1. Validation of empirical dew point as the upper limit for two-phase region

To characterize vacuum thermal stripping close to the empirical dew point and evaluate performance against previous literature, an initial experiment was conducted at 65 °C and 0.25 bar. This corresponded to the high mass transfer region identified along the pure water boiling curve (Fig. 4) (Ukwuani and Tao, 2016). At this condition, 98 %wt ammonia was stripped from the feed after 2.3 h (Fig. 5). The rate of ammonia removal declined over time, as the driving force for mass transfer became limiting (Eq. (5)). The volumetric mass transfer coefficient for ammonia was determined as 1.4 h^{-1} (Fig. A2). When normalised against the interfacial surface area of the stripping vessel (16 m^2 m^{-3}), this provided a mass transfer coefficient of 88 mm h^{-1}. This is in a similar range to published data for vacuum thermal stripping of real ammoniacal wastes (21-106 mm h^{-1}) at equivalent temperature and pressure along the pure water boiling curve (Table 3), despite differences in feed depth and mixing condition used in each study, which may influence the availability of dissolved ammonia at the liquid interface and thus the mass transfer driving force (Eq. 5) (Guida et al., 2022; Tao et al., 2019; Ukwuani and Tao, 2016). Ammonia removal had negligible impact on the mass fraction of water in the feed ($x_{H2O} > 0.998$), and therefore on water vapor pressure (Appendix A2). This was evidenced by the stable rate of water vaporization throughout (2 mol h^{-1}). Consequently, there was a decline in ammonia selectivity as the separation progressed (Fig. 5). At 65 °C, the equilibrium vapor pressures for water and ammonia were estimated to be 0.249 bar and 0.008 bar using Henry's Law, respectively (Fig. 6). Ammonia selectivity, therefore, is expected to be in the region of 0.03 which is in close agreement with the experimental results (Eq. 11). This evidences that the empirical dew point curve predicted for the solution was consistent with the feed saturation curve. Limited data is available for the composition of ammonia products from vacuum thermal stripping, as the vapor is typically delivered into a downstream acid scrubber for ammonia capture (Han et al., 2022; Tao et al., 2019, 2018; Ukwuani and Tao, 2016). In an example of vapor condensation, Guida et al. (2022) recovered 0.4 %wt aqueous ammonia after stripping a 0.6 g L^{-1} feed. In this work, a 2.1 %wt ammonia vapor was recovered after the same period of stripping. This is consistent with the higher initial feed concentration and therefore the higher ammonia vapor pressure during the separation (Bavarella et al., 2020).

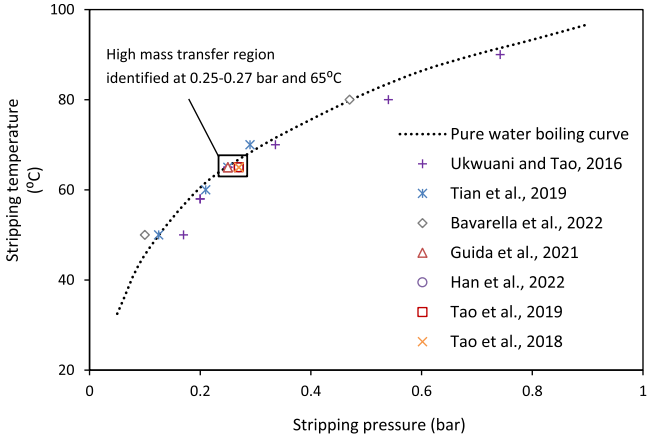

Fig. 4. Operating points for vacuum thermal stripping in previous work, placed within the context of the pure water boiling curve from 0-1 bar.

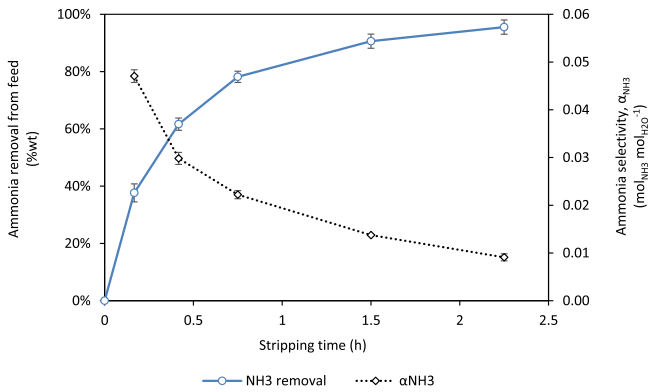

Fig. 5. Vacuum thermal stripping of synthetic wastewater at 65 °C and 0.25 bar. Operational conditions: $C_{NH3,0}$, 1.5 g L^{-1}; initial feed mass, 0.5 kg; pH, 11; condenser temperature, 3-5 °C.

3.2. Expanded two-phase region determined for selective ammonia separation

The stripping temperature was reduced from 65 to 61 °C at 0.25 bar to investigate the extent to which ammonia-water selectivity could be modified when transitioning across the two-phase region of the VLE. The rate of ammonia mass transfer was substantially influenced by the stripping temperature across this narrow range (Fig. 7a). Since the mass transfer driving force and the interfacial area were constant across all experiments, the direct influence of temperature on the ammonia mass transfer coefficient could be calculated (Eq. 6) (Salavera et al., 2005; Ukwuani and Tao, 2016). The mass transfer coefficient reduced from 88 mm h^{-1} at 65°C to 40 and 10 mm h^{-1} at 63°C and 61 °C, respectively (Fig. A2). Consequently, when compared after 1.5 h stripping then 91, 66 and 23 %wt ammonia removal was achieved at 65°C, 63°C and 61°C, respectively. Operating below the pure water boiling temperature (65 °C at 0.25 bar), and therefore below the activation energy threshold necessary for bulk evaporation, also greatly restricted water transport during stripping (Fig. 7b) (Prado and Vyazovkin, 2011). This is consistent with thermal stripping at atmospheric pressures where water vaporization reduced by an order of magnitude when temperature was reduced from 102 to 86 °C (Tao and Ukwuani, 2015). Since lowering the temperature had a disproportionately greater impact on the vaporization of water during stripping, it subsequently enhanced the selectivity for ammonia transport (Fig. 8). When stripping at 63 and 61 °C, an enhancement in ammonia selectivity of up to 1 and 2 orders of magnitude was observed, respectively, compared to 65 °C. Unlike stripping at 65 °C, the results strongly deviate from the theoretical selectivity based on the equilibrium vapor pressures of water and ammonia using Henry's Law ($\alpha_{NH3} \approx 0.033$-$0.034$). This highlights a discontinuity in the ammonia-water separation behavior when stripping below the dew point and entering the two-phase region. Interestingly, selective ammonia separation was demonstrated beyond the two-phase region initially proposed within the VLE, as estimated by extrapolation from ammonia-water mixtures across a higher concentration range relevant

Table 3
Literature comparison for vacuum stripping ammoniacal wastes at 0.25-0.27 bar close to the dew point of the feed.

Feed	$C_{NH3,0}$ g L^{-1}	η_{NH3} %	pH	T °C	HRT h	Depth[a] mm	Stirring -	k_La h^{-1}	k_L mm h^{-1}	Product	Reference
Synthetic wastewater	1.5	79%	11	65	0.8	60	Yes	1.4	88	2.1%wt $_{(v)c}$	This study
Synthetic wastewater	1.5	98%	11	65	2.3	60	Yes	1.4	88	0.9%wt $_{(v)c}$	
Synthetic wastewater	0.6	74%	10	65	0.8	60	Yes	1.7	106[b]	0.4%wt $_{(aq)c}$	Guida et al. (2022)
Ion exchange brine	0.6	44%	10	65	0.8	60	Yes	0.7	44[b]	0.4%wt $_{(aq)c}$	
Co-digestate	2.1	95%	9.5	65	6	180	No	0.5[b]	67[b]	$(NH_4)_2SO_4$ $_{(aq)}$	Han et al. (2022)
Hydrolysed urine	10	72%	9.3	65	12	200	No	0.1	21[b]	$(NH_4)_2SO_4$ $_{(aq)}$	Tao et al. (2019)
Municipal digestate	1	93%	9	65	5	170	No	0.6	100[b]	$(NH_4)_2SO_4$ $_{(aq)}$	Tao et al. (2018)
Dairy digestate	1.9	63%	9	65	5	170	No	0.2	32[b]	$(NH_4)_2SO_4$ $_{(aq)}$	
Dairy digestate	1.6	96%	9	65	1.5	23	No	0.6	37	$(NH_4)_2SO_4$ $_{(aq)}$	Ukwuani and Tao, (2016)
Municipal digestate	1.1	28%	9	65	2	180	No	0.2[b]	24[b]	$(NH_4)_2SO_4$ $_{(aq)}$	

T – temperature; P- pressure; HRT – hydraulic residence time.
[a] Feed depth estimated using on vessel data and fill volumes provided.
[b] Calculated based on data provided (Eq. 6).
[C] Ammonia concentration in recovered product.

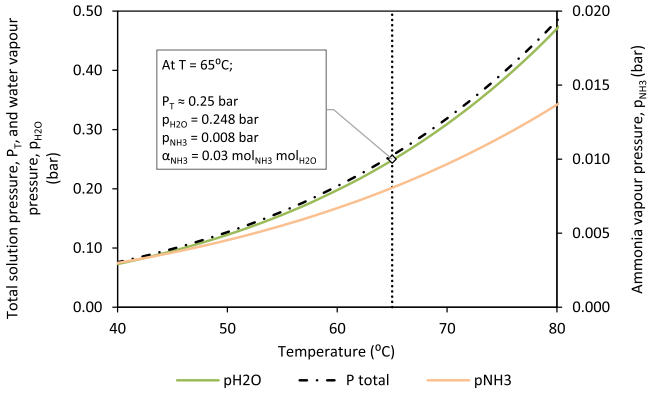

Fig. 6. Influence of temperature on the vapor pressure of water determined by Raoult's Law and of ammonia determined by Henry's Law for a 1.5 g L^{-1} ammonia solution (Appendix A2).

for absorption refrigeration (Pátek and Klomfar, 1995). In practice, solute-solvent interactions will affect the strength and type of intermolecular forces between ammonia and water, which can introduce uncertainty for individual component volatilities (Atkins and De Paula, 2006; Tan et al., 2004). Further complexity is introduced by the polar contribution of ammonia bonds which will influence interactive forces between molecules (Atkins and De Paula, 2006). These effects may be compounded by the highly dilute nature of the feed, therefore reducing the empirical predictability of the ammonia-water separation. Interestingly, the separation appears to conform more closely to the two-phase region bounded by the bubble point curve derived from Raoult's Law, which considers a mixture of two pure components (Fig. 9) (Appendix A2). A Raoult's Law approach predicts ammonia selectivity to be an order of magnitude greater due to the higher contribution of ammonia towards the total vapor pressure and is therefore a closer approximation for experimental selectivity measured at 63 and 61 °C. Reducing stripping temperature across this experimentally determined two-phase region enhances selectivity for ammonia, while simultaneously lowering the rate of ammonia mass transfer consistent with the principles of distillation. Whilst ammonia selectivity at 61 °C appears to have exceeded the theoretical limits of the VLE, the low vapor velocity at this condition may have facilitated partial water condensation and vapor rectification within the boundary of the reactor, analogous to the installation of a demister at the reactor outlet (Ukwuani and Tao, 2016).

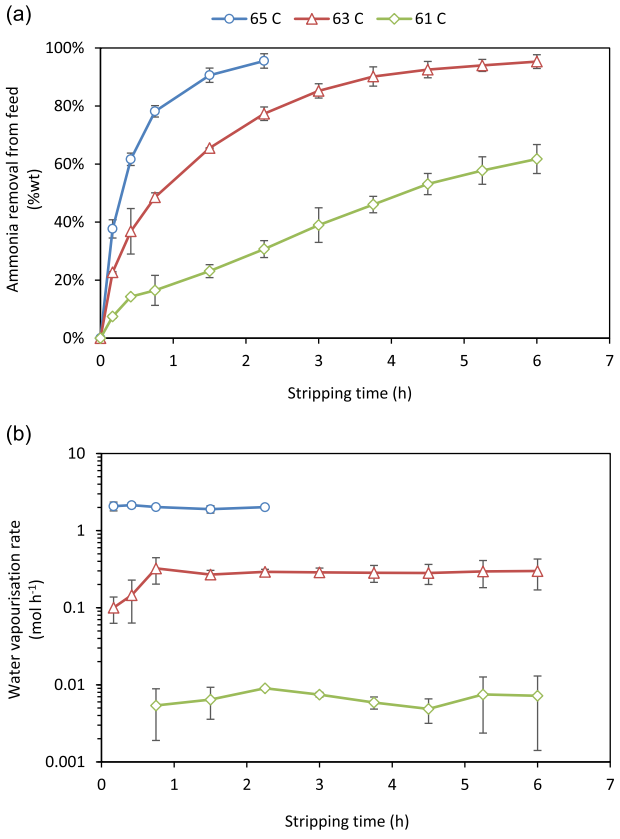

Fig. 7. Influence of temperature during vacuum thermal stripping of synthetic wastewater at 0.25 bar on (a) ammonia removal from the feed and (b) the water vaporization rate. Operational conditions: initial $C_{NH3,}$ 1.5 g L^{-1}; initial feed mass, 0.5 kg; pH, 11; condenser temperature, 3-5 °C.

3.3. Stripping within two-phase region supports ammonia to energy strategies

Manipulation of the stripping temperature within the two-phase region defined in this work could facilitate low energy, high purity ammonia recovery and has implications for ammonia to energy flowsheets within wastewater treatment. At 65 °C, low ammonia selectivity led to the production of vapor containing 1-5 %wt ammonia (Fig. 10a). Substantial water vaporization incurred a high latent heat penalty of up to 91 kWh_{th} kg_N^{-1} (Fig. 10b). The dilute vapor could be directly condensed to produce aqueous ammonia for utilisation in low temperature alkaline fuel cells (AFC) or for electrolytic hydrogen production

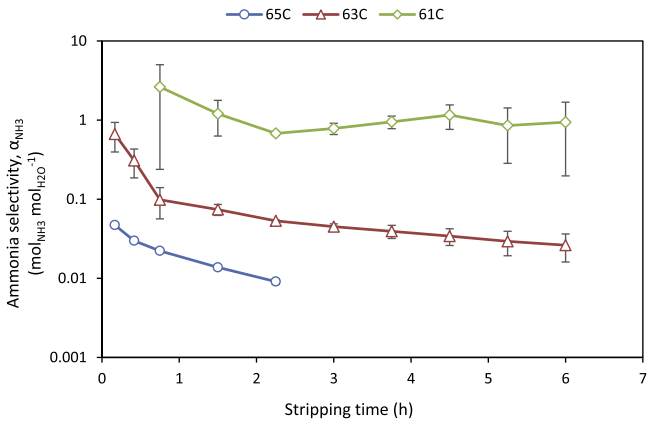

Fig. 8. Ammonia selectivity during vacuum thermal stripping of synthetic wastewater at 65, 63 and 61 °C and 0.25 bar. Operational conditions: initial C_{NH3}, 1.5 g L^{-1}; initial feed mass, 0.5 kg; pH, 11; condenser temperature, 3-5 °C.

(Table 1) (Davey et al., 2022; Lan and Tao, 2014; Vitse et al., 2005). Increasing the ammonia concentration will significantly enhance fuel cell power density or increase the rate of hydrogen evolution, therefore reducing cell size and cost (Cheddie, 2012; Davey et al., 2022; Zhang et al., 2020). This could be achieved by reducing the stripping temperature to 63 °C to generate concentrated ammonia vapor in the range 2-38 %wt. This is of sufficient quality to directly fuel a high efficiency solid oxide fuel cell (SOFC) which would avoid an intermediate condensation stage, liquid handling and the associated energy demand and exergy losses (van Linden et al., 2022). Alternatively, the addition of a downstream rectification stage could reduce the water content and increase the gas-phase ammonia concentration to enhance SOFC power density and expand options for energy generation (Teichgraber & Stein, 1994). Reduced water transport at 63 °C will limit the latent heat penalty below 35 kWh_{th} kg_N^{-1}. By further reducing the stripping temperature to 61 °C, a 43-64 % ammonia vapor was generated. Removal of the excess water vapor using a chiller or an advanced dehumidification process (e.g., desiccant coated heat exchanger) could produce a pure ammonia gas product to fuel an SOFC, co-fire a biogas turbine, be cracked into hydrogen or liquified to produce anhydrous ammonia (Venegas et al., 2021). Very high ammonia selectivity at 61 °C means that the production of the most energy dense and flexible ammonia product is associated with the lowest latent heat penalty (1 kWh_{th} kg_N^{-1}). This compares to 3-5 kWh_e kg_N^{-1} for mainstream biological nitrogen removal which is conventionally employed in wastewater treatment (Garrido et al., 2013; Wett, 2006). As a thermally driven process, vacuum stripping could recover sensible heat within the system boundary to reduce external heat demand. In the context of a centralised wastewater treatment works, waste heat sources are also available at an appropriate heat quality for use (e.g. biogas combustion in CHP engines). Where an extrinsic heat source is required, the cost for importing 1 unit of heat (kWh_{th}) is historically around four times lower than 1 unit of electricity (kWh_e) thus offering a potential cost benefit (Department for Business, Energy and Industrial Strategy, 2022). To overcome the limited rates of mass transfer during vacuum stripping at high selectivity, translation from a batch vessel to a continuous stripping column may be necessary. Packed columns will facilitate intensified rates of ammonia mass transfer by providing a high interfacial area. Vacuum thermal stripping close to the bubble point ($k_L = 10$ mm h^{-1}) in a packed column with an interfacial area of 400 m^2 m^{-3} could theoretically provide a volumetric mass transfer coefficient of 3.4 h^{-1}. Mass transfer could then become competitive with thermal air strippers (3-5 h^{-1}) employed commercially for ammonia removal from concentrated wastewaters (Guštin and Marinšek-Logar, 2011; Jiang, 2009; RVT, 2015).

3.4. Predictable ammonia-water separation behavior for wastewater

Vacuum thermal stripping was conducted using two centrates from full scale AD with different designs (Table 2), and the ammonia-water separation behavior compared to that achieved within synthetic wastewater. The intent of the validation was to confirm that vacuum stripping behaves comparably with a real wastewater where solution chemistry (e.g. salting out) and the presence of volatile species could modify selectivity. Vacuum stripping was compared close to the dew point (65 °C, 0.25 bar) since this offers the greatest mass transfer rate, and therefore the greatest risk of the co-transport of other species. Centrate A was produced from a conventional AD plant and comprised a dissolved ammonia concentration of 1.0 g L^{-1}, whereas Centrate B originated from an advanced AD (AAD) plant and had an ammonia concentration of 2.0 g L^{-1}. The higher ammonia concentration in Centrate B arises from the thermal hydrolysis of raw sludge in AAD. Thermal hydrolysis breaks down organic matter through intracellular lysis to

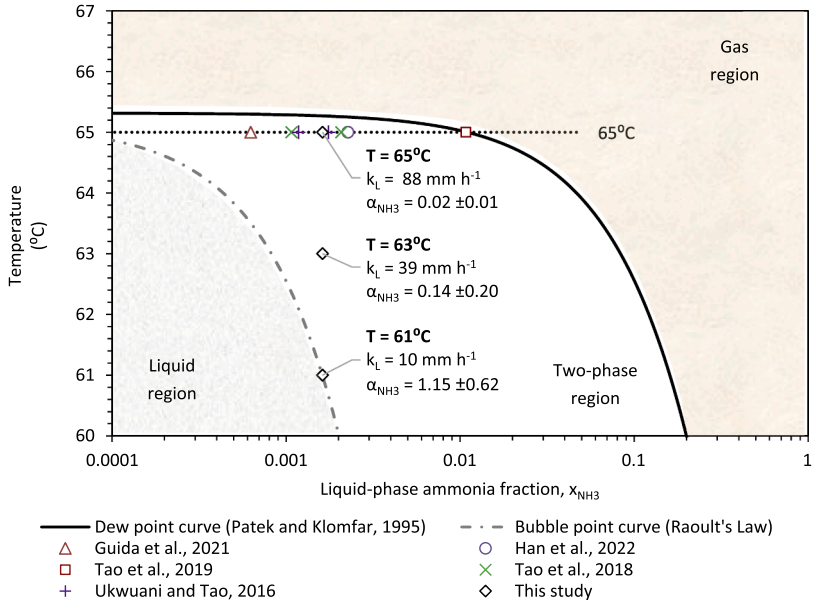

Fig. 9. Experimental ammonia vapor quality during transition through two-phase region plotted on VLE for NH_3-H_2O at 0.25 bar.

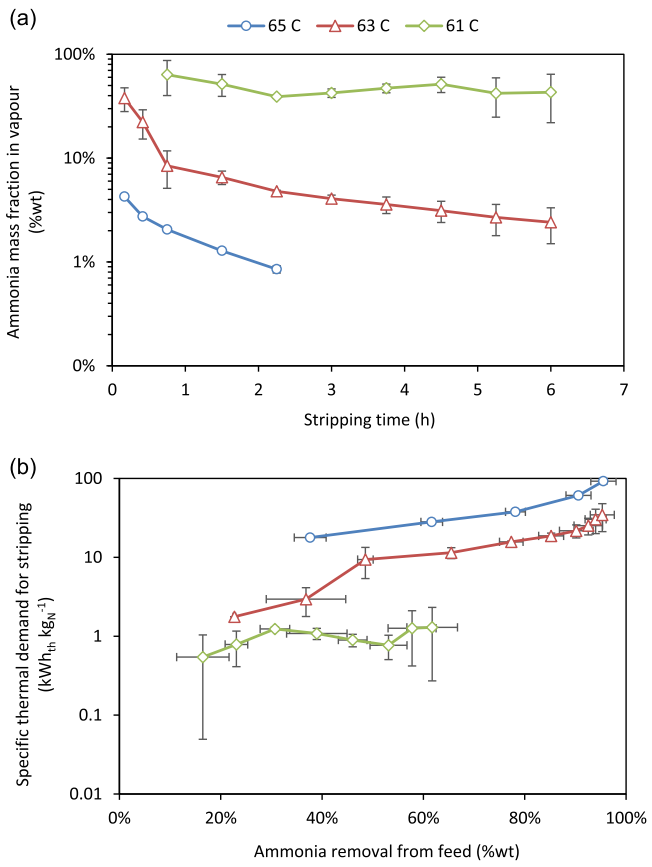

Fig. 10. Influence of temperature during vacuum thermal stripping of synthetic wastewater at 0.25 bar on (a) the mass fraction of ammonia in the vapor phase and (b) the specific thermal demand for ammonia stripping. Operational conditions: initial C_{NH3}, 1.5 g L^{-1}; initial feed mass, 0.5 kg; pH, 11; condenser temperature, 3-5 °C.

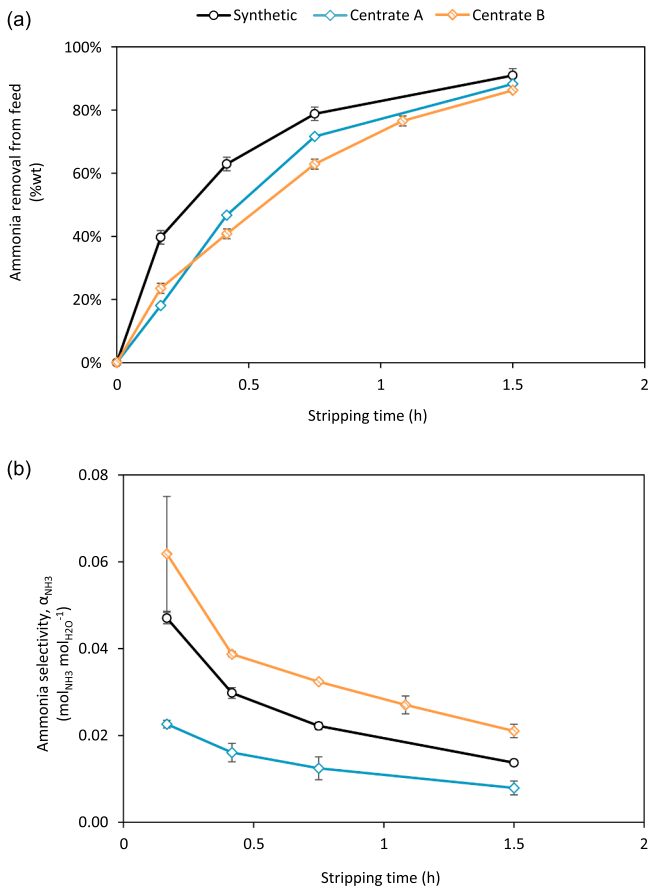

Fig. 11. (a) Ammonia removal and (b) ammonia selectivity over time during vacuum thermal stripping of synthetic wastewater, Centrate A and Centrate B at 65 °C and 0.25 bar. Operational conditions: initial feed mass, 0.5 kg; pH, 11; condenser temperature, 3-5 °C.

increase the availability of microbial nutrients and enhance biogas yield (Wilson and Novak, 2009). During this process, the dissolved ammonia concentration increases due to the conversion of organic nitrogen and the hydrolysis of proteins in the sludge (Ndam, 2017; Wilson and Novak, 2009). This disruption of cell and floc structure also alters the wider matrix chemistry which can increase the concentration of dissolved organic matter, gases and volatile compounds within the liquid-phase which could interact with the ammonia-water separation (Bougrier et al., 2008; Ndam, 2017). After 1.5 h stripping, 88 %wt and 86 %wt ammonia was removed from Centrate A and B, respectively (pH 11, Fig. 11a). Ammonia mass transfer coefficients were 95 and 87 mm h^{-1} for Centrate A and B, respectively, comparable to that of synthetic wastewater at the same condition (88 mm h^{-1}) (Fig. A3). A greater ammonia selectivity was observed for Centrate B, in line with its higher concentration and higher ammonia vapor pressure (Fig. 11b). Similar to stripping synthetic wastewater close to the dew point, the experimentally derived selectivity was in good agreement with theoretical values predicted by Henry's Law for Centrate A ($\alpha_{NH3} \approx 0.02$) and Centrate B ($\alpha_{NH3} \approx 0.04$). Consequently, the results indicate that despite the complex characteriztics and presence of other dissolved species within real wastewater, the ammonia-water separation behavior can be described through the binary VLE. After 1.5 h stripping, condensate produced from Centrate A had the lowest concentration (0.8 %wt) whilst condensate from Centrate B had the highest concentration (1.9 %wt) (Table 4). This reflected the higher initial concentration in Centrate B and therefore the greater driving force for ammonia mass transfer (Eq. 5). Both centrates yielded colourless condensate (Fig. A4). Interestingly, soluble COD of 0.42 and 0.24 g L^{-1} was present in condensate from Centrate A and Centrate B, respectively. This indicates that volatile organic compounds (VOCs) were co-transported during stripping. The presence of VOCs may explain why pH values were lower than expected, when compared against synthetic ammonia solutions of equivalent concentration (Davey et al., 2022). While further work is required, it may be possible to reduce VOC transfer by stripping within the two-phase region where water evaporation is limited to subsequently minimise product contamination. Mitigating the co-transport of dissolved compounds during stripping could have particular significance for the efficiency or lifetime for downstream generation technologies. For example, trace amounts of hydrogen sulphide (>1.0 mg m^{-3}) and siloxanes (>0.2 mg m^{-3}) which are present in wastewater can cause fatal cell degradation in SOFC (Papadias and Ahmed, 2012; Sasaki et al., 2011).

Table 4
Outcomes for vacuum thermal stripping synthetic and real wastewater for 1.5 h at 65 °C and 0.25 bar.

Parameter	Synthetic wastewater	Centrate A	Centrate B
Ammonia removal (%wt)	90%	88%	86%
k_L (mm h^{-1})	88	95	87
Ammonia fraction in condensate (% wt)	1.3%	0.8%	1.9%
Condensate pH (-)	12.2	9.8	10.5[a]
Condensate sCOD (g L^{-1})	-	0.42	0.24[a]

[a] Values originally published by Davey et al. (2022)

3.5. In-situ decarbonisation facilitates chemical-free vacuum thermal stripping

Raising the wastewater pH will increase the fraction of free ammonia and therefore favor mass transfer rate, selectivity and energy demand during vacuum thermal stripping (Fig. A1). Increasing Centrate A and B from pH 7.8 and 8.0 up to pH 11 demanded 135 and 275 mol_{NaOH} m^{-3}, respectively (Fig. A5). The increased chemical demand for Centrate B was consistent with its higher pH buffering capacity as indicated by alkalinity (Table 2). To overcome high buffering capacities within concentrated wastewaters, chemical addition for pH amendment will incur a substantive cost to ammonia recovery and is contrary to strategic roadmaps for net zero carbon and low chemical wastewater treatment (Water Europe, 2021; Water UK, 2020). Direct stripping of Centrate A and B without pH amendment was explored as an alternative treatment option (Fig. 12). Interestingly, both centrates exhibited a rapid increase in pH during vacuum thermal stripping at 65 °C and 0.25 bar. After 0.2 h, both feeds had increased above pH 9. After 1.5 h, a 67 % and 80 % decline in total inorganic carbon was observed for Centrate A and B, respectively, indicating that CO_2 desorption had occurred during stripping. Dissolved CO_2 contributes to wastewater acidity and decarbonisation by air stripping at low gas-liquid ratios has been previously explored for chemical-free pH amendment prior to ammonia stripping (Kang et al., 2017; Cohen & Kirchmann, 2004). In this work, a maximum pH of 9.4 was achieved during stripping. This is consistent with the bicarbonate equilibrium, which indicates that less than 0.01 % free CO_2 is available above pH 9.4, limiting further decarbonisation beyond this point (Bavarella et al., 2022; Kang et al., 2017). Thus, the increase in feed pH by CO_2 stripping enabled continuous ammonia stripping without pH amendment. After 1.5 h, 69 %wt and 65 %wt ammonia had been removed from Centrate A and B, respectively. Based on the stable trajectory of ammonia removal and the final pH (9.2) after 1.5 h, it is likely that ammonia removal would have continued if the experimental stripping period had been extended. However, the fraction of ammonia removal was lower than observed for Centrate A and B at initial pH 11 under the same stripping conditions after 1.5h (Fig. 11a). A lower rate of ammonia removal indicates that a lower fraction of free ammonia (Φ) was available during stripping, therefore reducing the mass transfer driving force (Eq. 5). This is consistent with the chemistry of ammonia speciation at 65 °C, which suggests that operating at pH 11 will release 100 % free ammonia whilst operating at pH 9 will release 92 % free ammonia (Fig. A1). In accordance with Le Châtelier's principle, the continuous removal of ammonia from solution will prompt the breakdown of ammonium and develop a dynamic chemical equilibrium (Eq. 1) (Licon Bernal et al., 2016). This enables ammonia removal to progress at a stable rate in systems where less than 100 % free ammonia is available at any time. The breakdown of ammonium is associated with the release of protons which can lower the solution pH. This was observed during ammonia extraction from batches of dilute wastewater using membrane contactors where regular addition of alkali was necessary to maintain a high pH and facilitate a consistent rate of mass transfer (Licon Bernal et al., 2016). In this work, pH values for Centrate A and B were relatively consistent despite progressive ammonia removal. This can be attributed to the high buffering capacity of centrate to resist pH change, which supported continuous chemical-free ammonia stripping from the complex wastewater matrix. The co-transport of CO_2 will yield a ternary gas phase. The CO_2-NH_3-H_2O ternary phase diagram is complex (Sutter et al., 2017), and can comprise solid product formation, including the formation of crystalline ammonium bicarbonate (Bavarella et al., 2022). Based on the ammonia-water mass balance, we propose that gas products formed across the two-phase region of the VLE are primarily within areas of the ternary phase diagram which preference formation of either gas or gas-liquid products, but further work should be conducted to relate product quality to solids formation mechanisms to mitigate risk of vacuum pump damage (which we did not observe during this study).

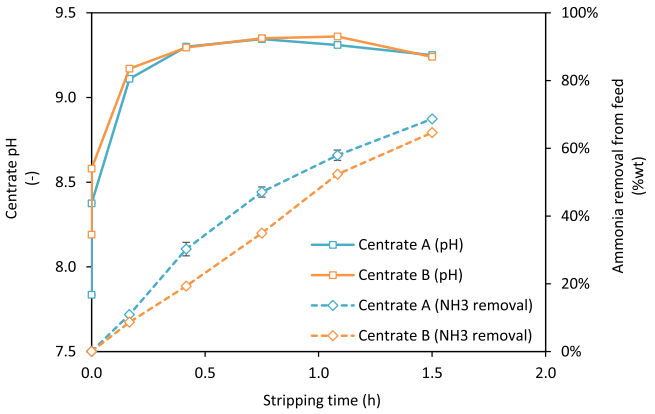

Fig. 12. Vacuum thermal stripping of Centrate A and Centrate B at their natural pH at 65 °C and 0.25 bar. Centrate A: initial C_{NH3}, 1.0 g L^{-1} and initial pH, 7.8. Centrate B: initial C_{NH3}, 2.0 g L^{-1} and initial pH, 8. Operational conditions: initial feed mass, 0.5 kg; pH measurements conducted at 21 °C.

4. Conclusion

This study provides the first experimental characterization of the vapor liquid equilibrium within the concentration range relevant to ammonia stripping. Vacuum stripping at the dew point provides mass transfer consistent with published data, and the ammonia selectivity closely corresponded to empirical modelling of the VLE. However, the two-phase region enables a substantial enhancement in ammonia selectivity. The mechanism introduced exposes an entirely new region in which to operate stripping that can reduce separation energy by two orders of magnitude versus current proposed approaches which can require multiple separation stages to achieve comparable product quality. Existing correlations poorly describe the lower limit of the two-phase region relevant for wastewater, since they are extrapolated from a considerably higher concentration range and cannot account for complex intermolecular forces arising from solute-solvent interactions involving polar ammonia. This study demonstrates it is possible to facilitate considerably richer ammonia gas product within this region that can be exploited as a net zero fuel with relatively minimal upgrading. Validation on real wastewater achieved comparable ammonia mass transfer for centrates of different origin indicating solution chemistry, and the presence of other components (e.g. VOCs) do not appreciably change the relative operating position within the VLE. In future work, vacuum stripping of real wastewater should be conducted at the lower boundary of the two-phase region to confirm separation is commensurate to that of the synthetic solution. Assessment on real wastewater confirmed vacuum enables simultaneous CO_2 degassing, raising pH sufficiently to enable chemical-free ammonia stripping. Vacuum stripping within the two-phase region can therefore produce a rich ammonia product relevant for the emerging ammonia and hydrogen economies through a chemical free and low energy processing route that offers a triple carbon benefit to the water sector.

Declaration of Competing Interest

The authors declare that they have no known competing financial interests or personal relationships that could have appeared to influence the work reported in this paper.

Data availability

I have provided a link to my data which is shared

Acknowledgments

We are grateful for the financial and technical support offered by Anglian Water, Northumbrian Water and Severn Trent Water. We also acknowledge the funding and training resources provided to Benjamin Luqmani from the Engineering and Physical Sciences Research Council through the STREAM Industrial Doctorate Centre. Data underlying this paper can be accessed at: https://doi.org/10.17862/cranfield.rd.22673926.v1.

Supplementary materials

Supplementary material associated with this article can be found, in the online version, at doi:10.1016/j.watres.2023.120856.

References

Anglian Water. (2021). Ofwat Breakthrough Challenge Success. https://www.anglianwater.co.uk/news/ofwat-breakthrough-challenge-success/(accessed 31/03/2023).

Anwar, S.W., Tao, W., 2016. Cost benefit assessment of a novel thermal stripping—acid absorption process for ammonia recovery from anaerobically digested dairy manure. Water Pract. Technol. 11, 355–364.

Atkins, P.W., De Paula, J., 2006. Atkin's Physical Chemistry. Oxford University Press, Oxford, UK, pp. 174–199, 8th ed.

Bates, R.G., Pinching, G.D., 1949. Acidic dissociation constant of ammonium Ion at 0 to 50°C and the base strength of ammonia. J. Res Nat. Bureau Stand. 42, 419–430.

Bates, R.G., Pinching, G.D., 1950. Dissociation constant of aqueous ammonia at 0 to 50° from E. m. f. studies of the ammonium salt of a weak acid. J. Am. Chem. Soc. 72, 1393–1396.

Bavarella, S., Hermassi, M., Brookes, A., Moore, A., Vale, P., Moon, I.S., Pidou, M., McAdam, E.J., 2020. Recovery and concentration of ammonia from return liquor to promote enhanced CO2 absorption and simultaneous ammonium bicarbonate crystallization during biogas upgrading in a hollow fibre membrane contactor. Sep. Purif. Technol. 241, 116631.

Bavarella, S., Luqmani, B., Thomas, N., Brookes, A., Moore, A., Vale, P., Pidou, M., McAdam, E.J., 2022. CO2 absorption into aqueous ammonia using membrane contactors: role of solvent chemistry and pore size on solids formation for low energy solvent regeneration. Sep. Purif. Technol. 290, 120786.

Bougrier, C., Delgenès, J.P., Carrère, H, 2008. Effects of thermal treatments on five different waste activated sludge samples solubilisation, physical properties and anaerobic digestion. Chem. Eng. J. 139, 236–244.

Campos, J.L., Valenzuela-Heredia, D., Pedrouso, A., Val Del Río, A., Belmonte, M., Mosquera-Corral, A., 2016. Greenhouse gases emissions from wastewater treatment plants: minimization, treatment, and prevention. J. Chem., 379635

Cesaro, Z., Ives, M., Nayak-Luke, R., Mason, M., Bañares-Alcántara, R., 2021. Ammonia to power: forecasting the levelized cost of electricity from green ammonia in large-scale power plants. Appl. Energy 282, 1–19.

Cheddie, D., 2012. Hydrogen Energy—Challenges and Perspectives. IntechOpen, London, UK, pp. 333–362, 1st ed.

Cooper, M., Botte, G.G., 2006. Hydrogen production from the electro-oxidation of ammonia catalyzed by platinum and rhodium on Raney nickel substrate. J. Electrochem. Soc. 153, A1894.

Davey, C.J., Luqmani, B., Thomas, N., McAdam, E.J., 2022. Transforming wastewater ammonia to carbon free energy: integrating fuel cell technology with ammonia stripping for direct power production. Sep. Purif. Technol. 289, 120755.

Dekker, N.J.J., Rietveld, G., 2006. Highly efficient conversion of ammonia in electricity by solid oxide fuel cells. J. Fuel Cell Sci. Technol. 3, 499–502.

Department for Business Energy and Industrial Strategy. (2021). UK Hydrogen Strategy. https://assets.publishing.service.gov.uk/government/uploads/system/uploads/attachment_data/file/1011283/UK-Hydrogen-Strategy_web.pdf (accessed 31/03/2023).

Department for Business Energy and Industrial Strategy. (2022). Gas and Electricity Prices in the Non-Domestic Sector. https://www.gov.uk/government/statistical-data-sets/gas-and-electricity-prices-in-the-non-domestic-sector (accessed 31/03/2023).

EC (European Community), 2008. 2008/98/EC of 19 November 2008 on waste and repealing certain Directives. Off. J. Eur. Union 3–30. https://eur-lex.europa.eu/legal-content/EN/TXT/PDF/?uri=CELEX:32008L0098&from=EN/3E. accessed 31/03/2023.

EEC Council, 1991. 91/271/EEC of 21 May 1991 concerning urban waste-water treatment. Off. J. Eur. Communities 40–52. https://eur-lex.europa.eu/legal-content/en/ALL/?uri=CELEX:31991L0271. accessed 31/03/2023.

Ganesh, N.S., Srinivas, T, 2017. Development of thermo-physical properties of aqua ammonia for Kalina cycle system. Int. J. Mater. Prod. Technol. 55, 113–141.

Garrido, J.M., Fdz-Polanco, M., Fdz-Polanco, F., 2013. Working with energy and mass balances: a conceptual framework to understand the limits of municipal wastewater treatment. Water Sci. Technol. 67, 2294–2301.

Guida, S., Van Peteghem, L., Luqmani, B., Sakarika, M., McLeod, A., McAdam, E.J., Jefferson, B., Rabaey, K., Soares, A., 2022. Ammonia recovery from brines originating from a municipal wastewater ion exchange process and valorization of recovered nitrogen into microbial protein. Chem. Eng. J. 427, 130896.

Guštin, S., Marinšek-Logar, R., 2011. Effect of pH, temperature and air flow rate on the continuous ammonia stripping of the anaerobic digestion effluent. Process Saf. Environ. Prot. 89, 61–66.

Han, Y., Agyeman, F., Green, H., Tao, W., 2022. Stable, high-rate anaerobic digestion through vacuum stripping of digestate. Bioresour. Technol. 343, 126133.

Heile, S., Chernicharo, C.A.L., Brandt, E.M.F., McAdam, E.J., 2017. Dissolved gas separation for engineered anaerobic wastewater systems. Sep. Purif. Technol. 189, 405–418.

Henze, M., Comeua, Y., Henze, M., 2008. Wastewater characterization. In: van Loosdrecht, M.C.M., Ekama, G.A., Brdjanovic, D. (Eds.), Biological Wastewater Treatment: Principles, Modelling and Design. IWA Publishing, London, UK, pp. 33–52, 1st ed.

Hewlett, S.G., Pugh, D.G., Valera-Medina, A., Giles, A., Runyon, J., Goktepe, B., Bowen, P.J., 2020. Industrial wastewater as an enabler of green ammonia to power via gas turbine technology. In: Proceedings of the ASME Turbo Expo 2020: Turbomachinery Technical Conference and Exposition. London, UK.

Hewlett, S.G., Valera-Medina, A., Pugh, D.G., Bowen, P.J., 2019. Gas turbine co-firing of steelworks ammonia with coke oven gas or methane: a fundamental and cycle analysis. In: Proceedings of the ASME Turbo Expo 2019: Turbomachinery Technical Conference and Exposition. Phoenix, AZ, USA.

Huang, J., Shang, C., 2006. Air Stripping. In: Wang, L.K., Hung, Y., Shammas, N.K. (Eds.), Advanced Physicochemical Treatment Processes. The Humana Press Inc., Totowa, NJ, USA, pp. 47–79, 1st ed.

International Energy Agency. (2021). Ammonia Technology Roadmap. https://iea.blob.core.windows.net/assets/6ee41bb9-8e81-4b64-8701-2acc064ff6e4/AmmoniaTechnologyRoadmap.pdf (accessed 31/03/2023).

Jackson, C., Fothergill, K., Gray, P., Haroon, F., Makhloufi, C., Kezibri, N., Davey, A., Lhote, O., Zarea, M., Davenne, T., Greenwood, S., Huddart, A., Makepeace, J., Wood, T., David, B., and Wilkinson, I. (2015). Ammonia to Green Hydrogen Project. https://assets.publishing.service.gov.uk/government/uploads/system/uploads/attachment_data/file/880826/HS420_-_Ecuity_-_Ammonia_to_Green_Hydrogen.pdf (accessed 31/03/2023).

Jamaludin, Z., Rollings-Scattergood, S., Lutes, K., Vaneeckhaute, C., 2018. Evaluation of sustainable scrubbing agents for ammonia recovery from anaerobic digestate. Bioresour. Technol. 270, 596–602.

Jiang, A. (2009). Ammonia Recovery from Digested Dairy Manure as Nitrogen Fertilizer. PhD thesis. Washington State University.

Kang, J., Kwon, G., Nam, J.H., Kim, Y.O., Jahng, D, 2017. Carbon dioxide stripping from anaerobic digestate of food waste using two types of aerators. Int. J. Environ. Sci. Technol. 14, 1397–1408.

Kurata, O., Iki, N., Matsunuma, T., Inoue, T., Tsujimura, T., Furutani, H., Kobayashi, H., Hayakawa, A., 2017. Performances and emission characteriztics of NH3-air and NH3-CH4-air combustion gas-turbine power generations. Proc. Combust. Inst. 36, 3351–3359.

Lan, R., Tao, S., 2014. Ammonia as a suitable fuel for fuel cells. Front. Energy Res. 2, 1–4.

Licon Bernal, E.E., Maya, C., Valderrama, C., Cortina, J.L, 2016. Valorization of ammonia concentrates from treated urban wastewater using liquid-liquid membrane contactors. Chem. Eng. J. 302, 641–649.

Mission Possible Partnership. (2022). Making net-zero ammonia possible. https://missionpossiblepartnership.org/wp-content/uploads/2022/09/Making-1.5-Aligned-Ammonia-possible.pdf (accessed 31/03/2023).

Moore, A., Auty, D, 2013. Digestion and greenhouses—synergistic resource recovery. In: 18th European Biosolids & Organic Resources Conference & Exhibition. Manchester, UK.

Morgan, E.R., 2013. PhD Thesis.

Nayak-Luke, R., Bañares-Alcántara, R., Wilkinson, I., 2018. "Green" ammonia: impact of renewable energy intermittency on plant sizing and levelized cost of ammonia. Ind. Eng. Chem. Res. 57, 14607–14616.

Ndam, N.E., 2017. PhD thesis.

Okafor, E.C., Kurata, O., Yamashita, H., Inoue, T., Tsujimura, T., Iki, N., Hayakawa, A., Ito, S., Uchida, M., Kobayashi, H., 2021. Liquid ammonia spray combustion in two-stage micro gas turbine combustors at 0.25 MPa; Relevance of combustion enhancement to flame stability and NOx control. Appl. Energy Combust. Sci. 7, 100038.

Organics Group. (2020). Removal, recovery and re-use of ammoniacal nitrogen from wastewater for power generation. https://organicsgroup.com/recovery-and-re-use-of-of-ammonia/(accessed 31/03/2023).

Papadias, D., and Ahmed, S. (2012). Biogas impurities and cleanup for fuel cells. Biogas and Fuel Cells Workshop, Golden, CO, USA.

Parliamentary Office of Science and Technology. (2007). Energy and Sewage, Postnote number 282,. http://www.parliament.uk/documents/post/postpn282.pdf (accessed 31/03/2023).

Pátek, J., Klomfar, J., 1995. Simple functions for fast calculations of selected thermodynamic properties of the ammonia-water system. Int. J. Refrig. 18, 228–234.

Patel, H.C., Woudstra, T., Aravind, P.V., 2012. Thermodynamic analysis of solid oxide fuel cell gas turbine systems operating with various biofuels. Fuel Cells 12, 1115–1128.

Prado, J.R., Vyazovkin, S., 2011. Activation energies of water vaporization from the bulk and from laponite, montmorillonite, and chitosan powders. Thermochim. Acta 524, 197–201.

Puigdomenech I., Plyasunov A. V., Rard J. A. and Grenthe I. (1997). Temperature corrections to thermodynamic data and enthalpy calculations. In: I. Grenthe and I. Puigdomenech (eds). Modelling in Aquatic Chemistry. OECD Nuclear Energy Agency, (https://www.nea.fr): Paris, pp. 427–493.

Raghuvanshi, S., Maheshwari, G., 2011. Analysis of ammonia–water (NH3-H2O) vapor absorption refrigeration system based on first law of thermodynamics. Int. J. Sci. Eng. Res. 2, 1–7.
RVT. (2015). Ammonia recovery Removal from liquids and gases. https://www.rvtpe.net/wp-content/uploads/prospekte/RVT_Ammonia_Recovery_120529.pdf (accessed 31/03/2023).
Salavera, D., Chaudhari, S.K., Esteve, X., Coronas, A., 2005. Vapor-liquid equilibria of ammonia + water + potassium hydroxide and ammonia + water + sodium hydroxide solutions at temperatures from (293.15 to 353.15) K. J. Chem. Eng. Data 50, 471–476.
Sasaki, K., Haga, K., Yoshizumi, T., Minematsu, D., Yuki, E., Liu, R.-R., Uryu, C., Oshima, T., Taniguchi, S., Shiratori, Y., Ito, K., 2011. Impurity poisoning of SOFCs. ECS Trans. 35, 2805–2814.
Siddiqui, O., Dincer, I., 2019. Development and performance evaluation of a direct ammonia fuel cell stack. Chem. Eng. Sci. 200, 285–293.
Sutter, D., Gazzani, M., Pérez-Calvo, J.F., Leopold, C., Milella, F., Mazzotti, M., 2017. Solid formation in ammonia-based processes for CO2 capture—turning a challenge into an opportunity. In: 13th International Conference on Greenhouse Gas Control Technologies. Lausanne, Switzerland.
Tan, T.C., Chai, C.M., Tok, A.T., Ho, K.W., 2004. Prediction and experimental verification of the salt effect on the vapor-liquid equilibrium of water-ethanol-2-propanol mixture. Fluid Phase Equilib. 218, 113–121.
Tao, W., Bayrakdar, A., Wang, Y., Agyeman, F, 2019. Three-stage treatment for nitrogen and phosphorus recovery from human urine: hydrolysis, precipitation and vacuum stripping. J. Environ. Manage. 249, 109435.
Tao, W., Ukwuani, A.T., 2015. Coupling thermal stripping and acid absorption for ammonia recovery from dairy manure: ammonia volatilization kinetics and effects of temperature, pH and dissolved solids content. Chem. Eng. J. 280, 188–196.
Tao, W., Ukwuani, A.T., Agyeman, F, 2018. Recovery of ammonia in anaerobic digestate using vacuum thermal stripping—acid absorption process: scale-up considerations. Water Sci. Technol. 78, 878–885.
Teichgraber, B., Stein, A., 1994. Nitrogen elimination from sludge treatment reject water—comparison of the steam-stripping and denitrification processes. Water Sci. Technol. 30, 41–51.
The Royal Society. (2020). Ammonia: zero-carbon fertiliser, fuel and energy store. Policy Briefing. https://royalsociety.org/topics-policy/projects/low-carbon-energy-programme/green-ammonia/(accessed 31/03/2023).
Ukwuani, A.T., Tao, W., 2016. Developing a vacuum thermal stripping—acid absorption process for ammonia recovery from anaerobic digester effluent. Water Res. 106, 108–115.
van Linden, N., Spanjers, H., van Lier, J.B., 2022. Fuelling a solid oxide fuel cell with ammonia recovered from water by vacuum membrane stripping. Chem. Eng. J. 428, 131081.
Vaneeckhaute, C., Lebuf, V., Michels, E., Belia, E., Vanrolleghem, P.A., Tack, F.M.G., Meers, E., 2017. Nutrient recovery from digestate: systematic technology review and product classification. Waste Biomass Valoriz. 8, 21–40.
Venegas, T., Qu, M., Nawaz, K., Wang, L, 2021. Critical review and future prospects for desiccant coated heat exchangers: materials, design, and manufacturing. Renew. Sustain. Energy Rev. 151, 111531.
Vitse, F., Cooper, M., Botte, G.G., 2005. On the use of ammonia electrolysis for hydrogen production. J. Power Sources 142, 18–26.
Wang, Z., Li, S., Zhang, C., Wang, D., Li, X., 2021. The opportunities and challenges for NH3 oxidation with 100% conversion and selectivity. Catal. Surv. Asia 25, 103–113.
Water Europe. (2021). Unleash the Potential of the Water-Energy Nexus in the Energy Efficiency Directive Joint Declaration. https://watereurope.eu/wp-content/uploads/Joint-Declaration-EU-ASE-.-WE-2.pdf (accessed 31/03/2023).
Water UK. (2020). Net Zero 2030 Routemap. https://www.water.org.uk/routemap2030 (accessed 31/03/2023).
Wett, B., 2006. Solved upscaling problems for implementing deammonification of rejection water. Water Sci. Technol. 53, 121–128.
Wilson, C.A., Novak, J.T., 2009. Hydrolysis of macromolecular components of primary and secondary wastewater sludge by thermal hydrolytic pretreatment. Water Res. 43, 4489–4498.
Winter, P., Pearce, P., Colquhoun, K., 2012. Contribution of nitrous oxide emissions from wastewater treatment to carbon accounting. J. Water Clim. Change 3, 95–109.
Zeng, L., Mangan, C., Li, X., 2006. Ammonia recovery from anaerobically digested cattle manure by steam stripping. Water Sci. Technol. 54, 137–145.
Zhang, M., Zou, P., Jeerh, G., Chen, S., Shields, J., Wang, H., Tao, S., 2020. Electricity generation from ammonia in landfill leachate by an alkaline membrane fuel cell based on precious-metal-free electrodes. ACS Sustain. Chem. Eng. 8, 12817–12824.